ELSEVIER

Journal of Alloys and Compounds 452 (2008) 254–257

Journal of ALLOYS AND COMPOUNDS

www.elsevier.com/locate/jallcom

Structure of new metastable cubic TbO_{2-x}

Faraz Ahmadpour, Yurij Mozharivskyj *

Department of Chemistry, McMaster University, 1280 Main Street West, Hamilton, Ont., Canada L8S 4M1

Received 6 September 2006; received in revised form 27 October 2006; accepted 2 November 2006
Available online 4 December 2006

Abstract

A new structure of TbO_{2-x} with the $Ia\bar{3}$ space group has been solved using single crystal diffraction techniques. From the structure refinement, a significant deficiency is found on one of the two oxygen sites which results in the $TbO_{1.68\,(6)}$ composition. Two types of Tb atoms with different bond valence sums and thus with two oxidation states exist in the structure. The phase does not obey the stability rules formulated for other oxygen deficient R_nO_{2n-2m} phases with R = Ce, Pr and Tb. The phase was obtained at high temperatures and is unstable at room temperature.

Keywords: Oxide material; Disordered system; Valence fluctuations; X-ray diffraction

1. Introduction

A number of oxygen-deficient TbO_{2-x} phases are known to exist due to the accessibility of +3 and +4 oxidation states for Tb. Structures of terbium oxide as well as those of analogous mixed valence Pr and Ce oxides are derived from the parent fluorite-type RO_2 structures (R = Ce, Pr and Tb, Fig. 1) by creating vacancies on the oxygen sites [1]. Since a vacancy carries a positive charge, repulsive energy makes any fluorite-type subcell with more than two vacant oxygen sites or with two closely located vacancies unstable in the composition range under analysis. As a consequence of this repulsive force, the following structural rules were formulated for the oxygen-deficient phases: (1) no $1/2\langle 1\,0\,0\rangle_F$ and $1/2\langle 1\,1\,0\rangle_F$ oxygen vacancy pairs could be present (the subscript F indicates the fluorite subcell) and (2) no $1/2\langle 1\,1\,1\rangle_{FF}$ oxygen vacancy pairs could occur across empty cubes (i.e. without an R atom between the vacancies) in a subcell [2]. The fact that every stable superstructure in these materials must contain an integral number of vacancies led to the formulation of the general R_nO_{2n-2m} formula which describes compositions of known phases with $n = (m =)$ 7 (1), 9 (1), 11 (1), 12 (1), 16 (1), 19 (2), 24 (2), 29 (3), 39 (4), 40 (4), 48 (4), 62 (6) and 88 (8) [1]. Structural features of RO_{2-x} were investigated using electron diffraction techniques, only structures and compositions of Ce_7O_{12} [3], Pr_7O_{12} [4], Pr_9O_{16} [5], $Pr_{10}O_{18}$ ($Pr_{40}O_{72}$) [6], $Pr_{12}O_{22}$ ($Pr_{24}O_{44}$) [7], Tb_7O_{12} and $Tb_{11}O_{20}$ [8] were verified through neutron powder diffraction.

An R_8O_{14} phase with $n = 8$ and $m = 1$ (one vacancy per subcell) has never been reported for pure Ce, Pr, or Tb oxides. If the cubic symmetry is assumed then the smallest unit cell for R_8O_{14} (or $R_4O_7 = RO_{1.75}$) is the one with $a = 2a_F$. The ordering of the vacancy pairs along $\langle 1\,1\,1\rangle_F$ can result in the formation of a cubic pyrochlore-type $A_2B_2O_7$ structure of the $Fd3m$ symmetry or a hypothetical $A_2B_2O_7$ structure of the $Pa3$ symmetry (A and B are two sites for metal atoms) [2]. The two structures can be also obtained by proper population of the vacant 16*c* sites in the so-called C-type R_2O_3 structure ($Ia\bar{3}$ space group, $a = 2a_F$). If, however, the vacancies were not ordered, then the symmetry of R_8O_{14} would be the same as of the C-type structure, i.e. $Ia\bar{3}$. To our knowledge, the structures with the $Fd3m$ and $Pa3$ symmetries have not been obtained yet. On the other hand, the $Ia\bar{3}$ space group has been observed in the mixed (R, R′)O_{2-x} oxides (R and R′ are tetra- and trivalent elements), e. g. for a CeO_2–$YO_{1.5}$ solid solution [2]. In case of the CeO_2–$YO_{1.5}$ phases, oxygen vacancies on the 16*c* site have been assumed on the basis of interatomic distances obtained from the single crystal data.

In case of pure rare-earth oxides, the $Ia\bar{3}$ structure, a possible R_8O_{14} (or $R_4O_7 = RO_{1.75}$) representative of the R_nO_{2n-2m} series, was observed only for TbO_{2-x} and only during the TEM studies. [9] While being investigated using electron diffraction

* Corresponding author at: ABB 423, Department of Chemistry, McMaster University, 1280 Main Street West, Hamilton, Ont., Canada L8S 4M1.
Tel.: +1 905 525 9140x27796; fax: +1 905 521 2773.
E-mail address: mozhar@mcmaster.ca (Y. Mozharivskyj).

0925-8388/$ – see front matter © 2006 Elsevier B.V. All rights reserved.
doi:10.1016/j.jallcom.2006.11.018

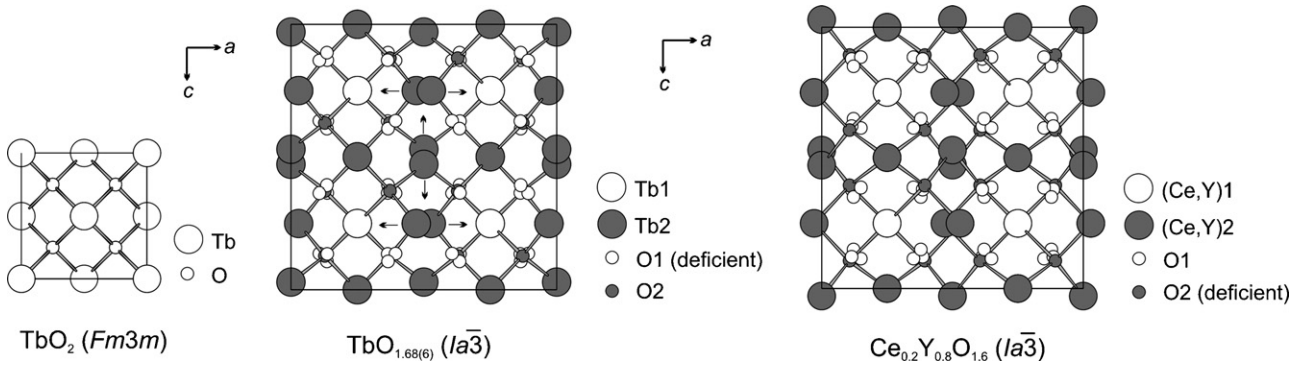

Fig. 1. Projections of the TbO_2 (fluorite-type), $TbO_{1.68\,(6)}$ and $Ce_{0.2}Y_{0.8}O_{1.6}$ [2] structures on the *xz* plane. For $TbO_{1.68\,(6)}$ and $Ce_{0.2}Y_{0.8}O_{1.6}$, only the Tb–O bonds to the O2 atoms are shown. The arrows in the $TbO_{1.68\,(6)}$ structure indicate Tb2 shifts from the ideal fluorite-type positions.

techniques, a phase with the initial composition of $TbO_{1.75–1.82}$ (as estimated from the average magnetic moment for Tb) has been observed to develop cubic superstructure with $a = 2a_F$ (10.6 (1) Å) from the parent fluorite structure due to oxygen depletion. Based on the electron diffraction images, the superstructure has been unambiguously assigned the $Ia\bar{3}$ space group, but no further structural analysis has been reported [9].

While exploring synthesis of novel Tb–Sb–N phases through the NaCl flux, we accidentally obtained silver-looking crystals of TbO_{2-x} with the $Ia\bar{3}$ symmetry and $a = 2a_F$. This paper reports on the room-temperature crystal structure of this oxide for the first time.

2. Experimental

2.1. Synthesis

Crystals of TbO_{2-x} were obtained during the exploratory synthesis of new Tb–Sb–N phases. Powders of Tb (CERAC, 99.9 wt.%), Sb (CERAC, 99.999 wt.%), $TbCl_3$ (Cerac, 99.9 wt.%) and NaN_3 (Alfa Aesar 99 wt.%) were combined in the 17:9:1:3 molar ratio with a total mass of 1g in a silica tube. One gram of NaCl (99.9 wt.%) was added as a flux, then the tube was evacuated and sealed. The mixture was heated to 1000 °C at the rate of 20 °C/h, kept at this temperature for 120 h and then cooled to 400 °C at the rate of 50 °C/h. The dominant phase was a black, moisture sensitive powder incorporated into the NaCl matrix. However, after detailed examination, three small terbium oxide crystals with metallic luster were extracted from the NaCl matrix. It is likely that the NaCl flux has facilitated oxygen extraction from the silica walls and its reaction with the Tb metal.

2.2. X-ray analysis

Room-temperature X-ray single crystal diffraction data for the two extracted crystals were collected on a STOE IPDSII image plate diffractometer with MoKα radiation and were harvested by taking 1° scans in ω in the full reciprocal sphere. Numerical absorption correction for both crystals were based on crystal face indexing, followed by a crystal shape optimization using program XSHAPE [10]. Indexing of the 4459 reflections collected yielded cubic lattice parameters within one standard deviation and analysis of the systematic absences unambiguously indicated the $Ia\bar{3}$ space group. Structure solution and refinement were done through programs SHELXS and SHELXL, respectively [11]. Atomic parameters for the two crystals were found to be identical within three standard deviations, so the structural data only for one of the crystal are presented here (Tables 1–4).

During the refinement, a large temperature factor was observed for the O1 site. Relaxing the occupancy for this site reduced the temperature factor by a factor of 2 and close to that of the O2 site. While vacancies on the O2 could not be excluded, the O2 site was assumed to be fully occupied. The refined composition based on the deficient O1 site is $TbO_{1.68\,(6)}$. In favor of the O1 deficiencies were also significantly longer distances between the O1 and Tb ions as compared to those between the O2 and Tb ions as vacancies on the O1 site carry a positive charge and should lead to longer Tb–O bonds. During the structure refinement in the $Ia\bar{3}$ space group, small pockets of extra electron density were found around the two O atoms: two peaks at 0.50 and 0.51 Å from O1 and one peak at 0.51 Å from O2. Treatment of oxygen thermal vibrations in either ellipsoidal or higher-order anharmonic approximations led to physically unreasonable vibrational surfaces. While introducing split, highly deficient O positions could account for this extra electron density, reducing the symmetry

Table 1
Crystal data and structure refinements for $TbO_{1.68\,(6)}$ ($T = 293$ (2) K, MoKα-radiation, graphite monochromator, the refinement method was full-matrix least-squares on F^2)

Space group	$Ia\bar{3}$ (no. 206)
Unit cell dimension, Å	10.710 (2)
Z	32
Density (calculated)	8.042 g/cm^3
Crystal dimensions	0.094 mm × 0.040 mm × 0.027 mm
2θ range	7.60–56.28°
Index ranges	$-14 \le h \le 13$, $-14 \le k \le 13$, $-14 \le l \le 14$
Reflections collected	4459 ($R\sigma = 0.0160$)
Independent reflections	254 ($R_{int} = 0.0518$)
Reflections with $I > 2\sigma(I)$	253
Completeness to max 2θ	99%
Data/restraints/par.	254/0/13
Goodness-of-fit on F^2	1.145
Final R indices [$F^2 > 2\sigma(F^2)$]	$R_1 = 0.0414$, $wR_2 = 0.0825$
Largest diff. peak/hole	1.911/−2.951 e/Å^3

$R_{int} = \sum \left| F_o^2 - F_o^2\,\text{mean} \right| / \sum F_o^2$; $R\sigma = \sum \sigma F_o^2 / \sum F_o^2$; $R_1 = \sum ||F_o| - |F_c|| / \sum |F_o|$; $R_w = \left(\sum w \times (F_o^2 F_c^2)^2 / \sum w \times (F_o^2)^2 \right)^{1/2}$, $w = 1/\sigma^2(F_o^2) + (a \times p)^2 + b \times P)$; $G_o F = \left(\sum w \times (F_o^2 - F_c^2)^2 / (n - p) \right)^{1/2}$ with $w = 1/(\sigma^2(F_o^2) + (a \times p)^2 + b \times p)$, where n is the number of observed reflections and p is number of parameters refined.

Table 2
Atomic coordinates and equivalent isotropic displacement parameters (U_{eq}, Å^2)

Atoms	Occup.	x	y	z	U_{eq}
Tb1, 8*b*	1	1/4	1/4	3/4	0.0074 (4)
Tb2, 24*d*	1	0.0289 (1)	0	1/4	0.0074 (3)
O1, 48*e*	0.79 (4)	0.3649 (21)	0.1064 (20)	0.3672 (21)	0.039 (7)
O2, 16*c*	1	0.1288 (16)	0.1288 (16)	0.1288 (16)	0.031 (6)

Table 3
Anisotropic displacement parameters for the Tb atoms

Atoms	U^{11}	U^{22}	U^{33}	U^{23}	U^{13}	U^{12}
Tb1	0.0074 (4)	0.0074 (4)	0.0074 (4)	0.0029 (4)	−0.0029 (4)	0.0029 (4)
Tb2	0.0091 (5)	0.0060 (5)	0.0070 (5)	0	0	0.0006 (4)

Table 4
Bond distances (Å) in $TbO_{1.68\,(6)}$

Atoms	Distance
Tb1–	
6O1	2.33 (2)
2O2	2.25 (2)
Tb2–	
2O1	2.38 (2)
2O1	2.39 (2)
2O1	2.44 (2)
2O2	2.175 (9)
O1–	
Tb1	2.33 (2)
Tb2	2.38 (2)
Tb2	2.39 (2)
Tb2	2.44 (2)
O2–	
Tb1	2.25 (2)
3Tb2	2.175 (9)

(to rhombohedral or orthorhombic) did not eliminate the pockets of this extra electron density.

After 2 months, the same crystals were tested again using single crystal diffraction techniques, and it was found that while strong reflections still corresponded to the original cubic cells, many extra reflections incommensurate with the original cells were also present. Since X-ray diffraction yields structural information of the entire crystal it is impossible to distinguish whether only the outer layers or the entire crystal underwent the structural transformation. This structural (and possibly compositional) instability might be the cause for physically unreasonable anisotropic thermal parameters for the oxygen atoms during the initial refinement, as some parts of the crystals might have already undergone transformation during the first data collections.

3. Discussion

The $Ia\bar{3}$ structure of $TbO_{1.68\,(6)}$ closely resembles that of TbO_2, the fluorite one (Fig. 1). The Tb1 coordinates of 1/4 1/4 1/4 and the O2 positions that are within three standard deviations from ideal "fluorite" positions of 1/8 1/8 1/8 reflect the underlying fluorite structure. On the other hand, the Tb2 and O1 shifts (Tb2 shifts in the *xz* plane are indicated by arrows in Fig. 1) from the ideal positions of 0 0 1/4 and 3/8 1/8 3/8 represent structural perturbations resulting, most likely, from oxygen deficiencies. We start our analysis of oxygen vacancies by examining the Tb–O distances (Table 4 and Fig. 2). Since oxygen vacancies carry positive charge, separation between Tb cations and oxygen-deficient sites should be larger than between Tb cations and fully occupied oxygen sites [1]. Significantly longer distances between the O1 and Tb ions as compared to those between the O2 and Tb ions clearly indicate concentration of vacancies on the O1 site (while vacancies on the O2 cannot be excluded, the O2 site is assumed to be fully occupied). In favor of

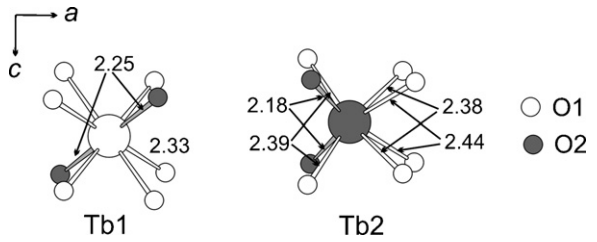

Fig. 2. Environment and bond distances for Tb1 and Tb atoms.

the O1 deficiencies was also the large isotropic temperature factor for this site during the single crystal refinement. In this light, the TbO_{2-x} phase is different from the CeO_2–$YO_{1.5}$ phases with the same space group where the vacancies are present on the O2 site (Fig. 1) [2]. In the CeO_2–$YO_{1.5}$ phases, the O2 vacancies result in pronounced shifts of the O2 atoms and significant elongation of the corresponding (Ce, Y)–O2 bonds. This difference may explain difficulties in obtaining the $TbO_{1.68\,(6)}$ structure, as the deficient O1 site (48*e*) and fully occupied O2 site (16*c*) cannot be obtained through the oxidation of Tb_2O_3 with fully occupied O1 and empty O2 sites [12].

As indicated before, the Coulomb repulsion between the Tb cations and oxygen vacancies results in the elongation of the Tb–O1 distances and the Tb2 cations being shifted from the ideal fluorite position of 0 0 1/4. The answer for why only the Tb2 cations move but not the Tb1 ones is found in the oxygen coordination around each terbium. While the Tb2 cations can shift away from the O1 sites towards O2 sites due to the two-fold symmetry of its oxygen environment, the Tb1 cations remained pinned at the ideal fluorite positions because of the $\bar{3}$ symmetry of its oxygen environment.

An analysis of bond valence sums, *V*, was carried out for the two Tb sites to obtain information on oxidation states of cations. The Tb atoms in $TbO_{1.68\,(6)}$ have mixed valency, and the averaged bond valence parameter for the Tb–O bonds had to be calculated first. Although there is no tabulated bond valence parameter for Tb^{+4}–O in the literature, the $R_{Tb-O}{}^{4+}$ value can be estimated from the R_{Ce-O} values taking into account similar crystallochemical behavior of cerium and terbium. The bond valence parameters for the Ce^{3+}–O and Ce^{4+}–O bonds are given by Brese and O'Keeffe [13], and their ratio $R_{Ce-O}{}^{3+}/R_{Ce-O}{}^{4+} = 2.151/2.028 = 1.061$ should be close to the $R_{Tb-O}{}^{3+}/R_{Tb-O}{}^{4+}$ ratio. In this way, a value of 2.049/1.061 = 1.931 is obtained for $R_{Tb-O}{}^{4+}$ (2.049 Å is $R_{Tb-O}{}^{3+}$ and is taken from [13]). In anionic approximation, the $TbO_{1.68}$ composition requires 64% of Tb^{3+} and 36% of Tb^{4+} for a charge balance, and this yields an average bond valence parameter, R_{Tb-O}, of 2.01 Å. The calculated bond valence sums are 3.55 and 3.34 for Tb1 and Tb2, respectively, and indicate a more oxidized state for Tb1. When these sums are taken as the Tb charges,

then the number of anionic species, i.e. oxygen atoms, comes to $(3.55 \times 8 + 3.34 \times 24)/2 = 54.3$ per cell. This result agrees well with 54 ± 2 achieved from the single crystal refinement, even despite the fact that the average bond valence parameter was used for the two Tb sites.

The Tb–O bond distances around Tb atoms can serve as a test for the charge assignment. The ionic radii for eight-coordinated Tb^{3+} and of Tb^{4+} and for four-coordinated O^{2-} taken from Shannon and Prewitt [14] were used to calculate average $Tb1^{3.55+}$–O and $Tb2^{3.35+}$–O bond distances. The values of 2.33 and 2.36 Å agree well with the average Tb1–O and Tb2–O distances of 2.31 and 2.35 Å obtained from the single crystal data. Based on this comparison as well as the analysis of the bond valence sums, the following conclusions can be drawn: (1) the two Tb sites have mixed valences, and (2) the Tb1 atoms are more oxidized.

We want to point out a short Tb2–O2 distance of 2.175 (9) Å in the $TbO_{1.68\,(6)}$ structure, where the rest of the bonds are 2.25 Å and longer. This particular bond is also shorter than the Tb^{4+}–O bond of 2.251 Å found in TbO_2 [15]. Although at this stage we have no rationale for the existence of such shorts bonds, we found that similarly short bonds are present in other mixed valence rare-earth oxides, e.g. 2.1589 (9) Å in Tb_7O_{12}, 2.153 (4) and 2.172 (4) Å in $Tb_{11}O_{22}$ [8], 2.148 (4) and 2.168 (4) Å in Pr_9O_{16} [5]. If the bond valence were calculated for such bonds using the literature-based bond valence parameters, then the oxygen valence would become significantly larger than 2. In case of O2 in the $TbO_{1.68\,(6)}$ structure, the bond valence sum would be 2.43, which clearly indicates that the assumed bonding scheme involving 4 strong O2–Tb interaction is not well suited here.

Any composition with an Tb:O ratio smaller than 1:1.75 indicates more than one vacancy, on average, in every fluorite-type subcell and therefore presence of $1/2\langle 1\,1\,0\rangle_F$ vacancy pairs and, possibly of $1/2\langle 1\,0\,0\rangle_F$ ones in addition to $1/2\langle 1\,1\,1\rangle_F$ ones depending on the symmetry and/or vacancy ordering. Combination of $1/2\langle 1\,1\,0\rangle_F$ and $1/2\langle 1\,1\,1\rangle_F$ vacancy pairs is observed in the C-type structure of R_2O_3 and stems from the 16*c* site being completely empty (the O2 site). In case of the TbO_{2-x} phase investigated, the 48*e* site (the O1 site) is statistically deficient and three types of vacancy pairs, $1/2\langle 1\,1\,1\rangle_F$, $1/2\langle 1\,1\,0\rangle_F$ and $1/2\langle 1\,0\,0\rangle_F$, may be present. Obviously, a $1/2\langle 1\,0\,0\rangle_F$ vacancy pair is most unstable due to a small charge separation and is less likely to occur. Still, even presence of a $1/2\langle 1\,1\,0\rangle_F$ vacancy pair violates the stability rules formulated for other oxygen deficient R_nO_{2n-2m} phases and, thus, the $Ia\bar{3}$ structure does not fall into this series.

The $Ia\bar{3}$ phase obtained by us is thermodynamically unstable in the air and/or at room temperature. As mentioned in the experimental section, after two months the same crystal was tested again using single crystal diffraction techniques, and it was found that many extra reflections incommensurate with the original cell were present. Due to the fact that X-ray diffraction yields structural information of the entire crystal, it is impossible to distinguish whether only the outer layers or the entire crystal underwent the structural transformation. Since the anomalous thermal behavior was associated only with the O atoms, it can be speculated that the structural (and possibly compositional) perturbations are likely to be driven by oxygen atoms. Although indirectly, extra electron density around the two oxygen atoms may also point at the dymanic nature of the oxygen sublattice.

Because of the limited number and small size of single crystals obtained we could not perform a quantitative compositional analysis of the $Ia\bar{3}$ phase using other analytical techniques. Our attempts to produce this phase by oxidizing Tb metal at different temperatures (up to 1350 °C) and for different periods of time were unsuccessful. Besides the temperature range at which the phase is thermodynamically stable, another unknown is oxygen pressure. The $TbO_{1.68\,(6)}$ composition obtained from the single crystal refinements indicates that the phase is rather oxygen poor and is likely to form in an oxygen-poor environment. The same can be concluded from the experiments performed by Malchus et al. [9], in which they observed formation of the $Ia\bar{3}$ structure from the initial $TbO_{1.75-1.82}$ phase as a result of oxygen depletion during the TEM experiments.

Acknowledgements

This work was supported by a Discovery Grant from the Natural Sciences and Engineering Research Council of Canada.

References

[1] Z.C. Kang, L. Eyring, J. Alloys Compd. 249 (1997) 206–212.
[2] N. Gabbitas, J.G. Thompson, R.L. Withers, A.D. Rae, J. Solid State Chem. 115 (1995) 23–36.
[3] S.P. Ray, D.E. Cox, J. Solid State Chem. 15 (1975) 333–343.
[4] R.B. Von Dreele, L. Eyring, A.L. Bowman, J.L. Yarnell, Acta Cryst. B31 (1975) 971–974.
[5] J. Zhang, R.B. Von Dreele, L. Eyring, J. Solid State Chem. 118 (1995) 133–140.
[6] J. Zhang, R.B. Von Dreele, L. Eyring, J. Solid State Chem. 118 (1995) 141–147.
[7] J. Zhang, R.B. Von Dreele, L. Eyring, J. Solid State Chem. 122 (1996) 53–58.
[8] J. Zhang, R.B. Von Dreele, L. Eyring, J. Solid State Chem. 104 (1993) 21–32.
[9] M. Malchus, M. Jansen, Solid State Sci. 2 (2000) 65–70.
[10] STOE, and Cie. X-SHAPE Version 2.05 and X-RED32 Version 1.10. STOE & Cie GmbH, Darmstadt, Germany.
[11] G.M. Sheldrick, SHELXL97 and SHELXS97, University of Gottingen, Germany, 1997.
[12] C. Boulesteix, L. Eyring, J. Solid State Chem. 75 (1988) 291–295.
[13] N.E. Brese, M. O'Keeffe, Acta Cryst. B47 (1991) 192–197.
[14] R.D. Shannon, C.T. Prewitt, Acta Cryst. B25 (1969) 925–946.
[15] D.M. Gruen, W.C. Koehler, J.J. Katz, J. Am. Chem. Soc. 73 (1951) 1475–1479.